Journal of Sound and Vibration (2002) **257**(4), 635–651
doi:10.1006/jsvi.5072, available online at http://www.idealibrary.com on IDEAL®

NATURAL VIBRATIONS OF LAMINATED COMPOSITE BEAMS BY USING MIXED FINITE ELEMENT MODELLING

G. S. Ramtekkar and Y. M. Desai

Department of Civil Engineering, Indian Institute of Technology Bombay, Powai, Mumbai 400 076, *India. E-mail: desai@civil.iitb.ac.in*

AND

A. H. Shah

Department of Civil Engineering, The University of Manitoba, Winnipeg, Man., Canada R3T 2N2

(*Received* 8 *October* 2001, *and in final form* 25 *February* 2002)

A six-node, plane-stress mixed finite element model has been developed by using Hamilton's energy principle for the natural vibrations of laminated composite beams. Continuity of the transverse stress and displacement fields has been enforced through the thickness of the laminated beam in the formulation for proper modelling. The transverse stress components have been invoked as the nodal degrees of freedom by applying elasticity relations. Natural frequencies of laminated composite beams obtained through the present formulation have been shown to be in good agreement with the data available in the literature. Various mode shapes have also been presented as benchmark solutions.

1. INTRODUCTION

Fiber-reinforced composites are finding increasing application in aerospace, marine, transportation, electrical, chemical, construction and consumer goods industries owing to their high strength-to-weight and stiffness-to-weight ratios. All these uses of composite materials in advanced technology areas, where precision and reliability play a paramount role, demand clear understanding of their behavior and performance under severe operating environment(s). Failure due to delamination is one of the important behavioral aspects, which needs prime attention. It has been concluded from investigations by Pipes and Pagano [1] and Rybicki [2] that high interlaminar stresses on the free edge of laminates cause edge delamination. A theory that can predict all these stresses accurately is certainly desired for a clear understanding of the failure mechanism involved in the delamination of laminated composites.

The behavior of composite laminates can be characterized by complex three-dimensional state of stress, evidencing high interlaminar stresses caused by the inherent anisotropy and mismatches of material properties of such structural members [3]. Elastic solutions for layered plates [4–6] indicate that interlaminar continuity of transverse normal and shear stresses as well as displacement fields through the thickness of the laminated plates are essential requirements for their analysis. Thus, a layer-wise analysis is often required for laminated composite structures. Various displacement-based layer-wise theories and finite element (FE) formulations have been proposed by Reddy [7], Soldatos

0022-460X/02/$35.00

[8], Wu and Kuo [9], Wu and Hsu [10] and others. These theories and the corresponding FE models have been reported to provide satisfactory results for both global (e.g., deflections and flexural stresses) and local values (e.g., transverse stresses) of thin and thick laminates. However, in all these models only the continuity of displacement fields through the thickness was satisfied. The continuity of transverse stress components at the interface could not be enforced.

A layer-wise mixed/hybrid FE model with displacement and transverse stress components as primary variables can easily satisfy the requirements of transverse stress continuity in addition to the continuity of displacement fields through the thickness of the laminated composite structure. Transverse stress components can be evaluated directly through such a mixed FE model. Thus, integration of the equilibrium equations can be avoided. This is helpful as they involve differentiation of in-plane stresses and displacement fields, thereby introducing further approximations in the calculation of transverse stresses. Wu and Lin [11], for example, presented a two-dimensional mixed FE scheme based on a local high order displacement model for the analysis of sandwich structure, where displacement continuity conditions at the interface between layers were regarded as the constraints and the interlaminar stresses were introduced as the Lagrange multiplier. Shi and Chen [12] also developed a three-dimensional mixed FE model based on global–local laminate variational model. The model proposed mixed use of a hybrid element within a high-precision stress solution region in the thickness direction of the laminate and a conventional displacement FE in the remaining. Carrera [13–15] has done extensive work on the development of mixed FE model. Firstly, a mixed plate element was developed [13] as an extension to C^{o} Reissner–Mindlin plate element by using Reissner's mixed variational principle, in which the zig-zag variation of in-plane displacement fields through the thickness was ensured by including additional terms in the standard Reissner–Mindlin displacement model whereas the transverse displacement field was kept unchanged. Stress degrees of freedom (d.o.f.) was introduced by assuming transverse shear stress fields. As a further development, Carrera [14, 15] also introduced the transverse normal stress field into the FE model. Because of the fact that in any mixed FE model developed by using Reissner's variational principle, the stress fields are assumed independent of the displacement fields, the fundamental elastic relations cannot be satisfied exactly.

A six-node, plane-stress mixed FE model has been developed in the present formulation, by using Hamilton's minimum energy principle. The transverse stress quantities (σ_z and τ_{xz}) are invoked as the nodal d.o.f. by using fundamental elastic relations between displacement and stress fields. This ensures the satisfaction of elastic equations throughout an elastic continuum, which is lacking in numerical models developed by using various mixed variational principles. Because the transverse stress components are themselves the nodal d.o.f. in the present FE model, their computation does not require integration of the equilibrium equations which otherwise would reduce the accuracy in their determination. Moreover, it can appropriately model a composite laminated structural member of any number of lay-ups of different materials as it satisfies exactly, the requirements of through thickness continuity of displacement as well as transverse stress fields.

2. FORMULATION

An anisotropic composite laminated beam consisting of N layers of orthotropic laminae shown in Figure 1(a,b) has been considered for FE analysis. The beam has been discretized

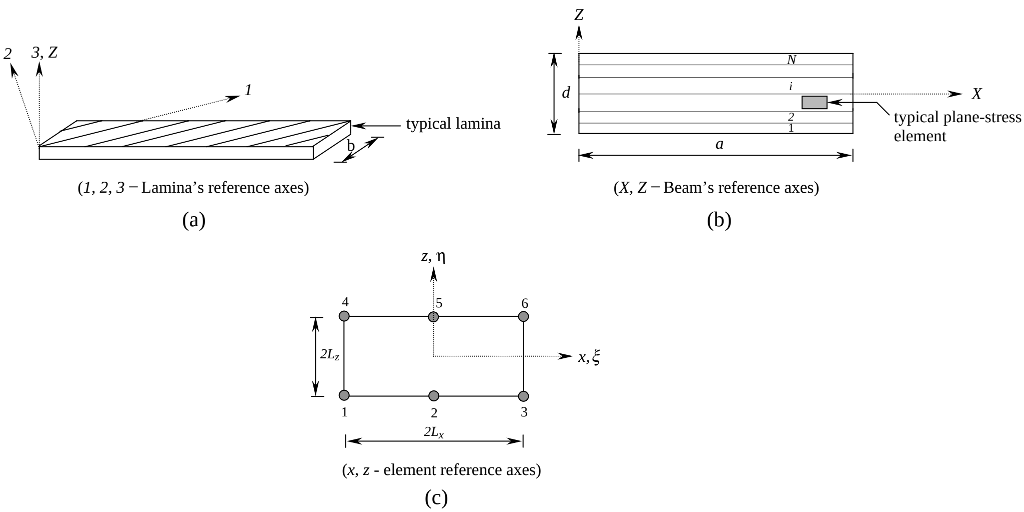

Figure 1. Geometry of laminated beam and mixed finite element.

into a number of plane-stress elements. Each element lies completely within a lamina; no element crosses the interface between any two successive laminae.

2.1. KINEMATICS

A six-node, plane-stress mixed finite element model shown in Figure 1(c) has been developed by considering the displacement fields $u(x, z, t)$ and $w(x, z, t)$ having quadratic variation along the longitudinal axis "x" and cubic variation along the transverse axis "z". The displacement fields can be expressed as

$$u_k(x, z) = \sum_{i=1}^{3} g_i a_{0ik} + z \sum_{i=1}^{3} g_i a_{1ik} + z^2 \sum_{i=1}^{3} g_i a_{2ik} + z^3 \sum_{i=1}^{3} g_i a_{3ik}, \quad k = 1, 2, \tag{1}$$

where

$$g_1 = \frac{\xi}{2}(\xi - 1), \quad g_2 = 1 - \xi^2, \quad g_3 = \frac{\xi}{2}(1 + \xi), \tag{2}$$

$$\xi = x/L_x \tag{3}$$

and

$$u_1(x, z, t) = u(x, z, t); \quad u_2(x, z, t) = w(x, z, t). \tag{4}$$

Further, the generalized co-ordinates a_{mik} ($m = 0, 1, 2, 3$; $i = 1, 2, 3$; $k = 1, 2$) are functions of element co-ordinate axis "z". The element's co-ordinate axes x, z are parallel to the laminate co-ordinate X, Z.

It may be noted that the variation of displacement fields has been assumed to be cubic along the thickness of element although there are only two nodes along the "z" axis of an element (Figure 1(c)). Such a variation is required for invoking transverse stress components σ_z and τ_{xz} as the nodal d.o.f. in the present formulation. Further, it also ensures parabolic variation of transverse stresses through the thickness of an element.

2.2. CONSTITUTIVE EQUATION

Each lamina in the laminate has been considered to be in the state of plane stress in X–Z plane so that the constitutive relation for a typical ith lamina with reference to the coordinate system can be shown to be

$$\{\sigma\} = [D]\{\in\}, \tag{5}$$

where

$$\{\sigma\} = [\sigma_x \ \ \sigma_z \ \ \tau_{xz}]^{\mathrm{T}}, \tag{6}$$

$$[D] = \begin{bmatrix} D_{11} & D_{13} & 0 \\ D_{13} & D_{33} & 0 \\ 0 & 0 & D_{55} \end{bmatrix}, \tag{7}$$

$$\{\in\} = [\in_x \ \ \in_z \ \ \gamma_{xz}]^{\mathrm{T}}. \tag{8}$$

The coefficients D_{mn} are the elastic constants.

2.3. FE FORMULATION

The transverse stresses can be obtained from the constitutive equation, equation (5) and strain–displacement relations as

$$\tau_{xz} = D_{55}\gamma_{xz} = D_{55}\left(\frac{\partial u}{\partial z} + \frac{\partial w}{\partial x}\right), \tag{9}$$

$$\sigma_z = D_{13} \in_x + D_{33} \in_z = D_{13}\frac{\partial u}{\partial x} + D_{33}\frac{\partial w}{\partial z}. \tag{10}$$

Equations (9) and (10), respectively, can be rearranged in the following form:

$$\left(\frac{\tau_{xz}}{D_{55}} - \frac{\partial w}{\partial x}\right) = \frac{\partial u}{\partial z} \tag{11}$$

$$\frac{1}{D_{33}}\left(\sigma_z - D_{13}\frac{\partial u}{\partial x}\right) = \frac{\partial w}{\partial z} \tag{12}$$

substituting equations (1), (11) and (12) at each node of the element, the following expressions for the displacement fields $u(x, z, t)$ and $w(x, z, t)$ can be obtained:

$$u(x,z,t) = \sum_{n=1}^{6} g_i\left(f_q u_n + f_p\frac{\partial u_n}{\partial z}\right), \tag{13}$$

$$w(x,z,t) = \sum_{n=1}^{6} g_i\left(f_q w_n + f_p\frac{\partial w_n}{\partial z}\right), \tag{14}$$

where "n" are the node numbers (1, 2, ..., 6) of the element, shown in Figure 1(c). u_n and w_n are the nodal displacement d.o.f. and $\partial u_n/\partial z$ and $\partial w_n/\partial z$ contain nodal transverse stress d.o.f. That is how nodal transverse stress terms (i.e., stress d.o.f.) are brought into the expression of displacement fields. Further,

$i=1, 2, 3$ for the nodes with $\xi = -1, 0$ and 1, respectively, $\eta = z/L_z$, $q=1, 2$, $p=3, 4$, for the nodes with $\eta=-1$ and 1, respectively,

$$f_1 = \tfrac{1}{4}(2 - 3\eta + \eta^3), \quad f_2 = \tfrac{1}{4}(2 + 3\eta - \eta^3),$$
$$f_3 = \frac{L_z}{4}(1 - \eta - \eta^2 + \eta^3), \quad f_4 = \frac{L_z}{4}(-1 - \eta + \eta^2 + \eta^3). \tag{15}$$

Equations (13) and (14) can be rewritten in the standard FE form as

$$\{u\} = [u\ w]^{\mathrm{T}} = [N]\{q\}, \tag{16}$$

where

$$[N] = [\underline{N}_1\ \ \underline{N}_2\ \ \underline{N}_3\ \ \underline{N}_4\ \ \underline{N}_5\ \ \underline{N}_6], \tag{17}$$

$$\{q\} = [\underline{q}_1^{\mathrm{T}}\ \ \underline{q}_2^{\mathrm{T}}\ \ \underline{q}_3^{\mathrm{T}}\ \ \underline{q}_4^{\mathrm{T}}\ \ \underline{q}_5^{\mathrm{T}}\ \ \underline{q}_6^{\mathrm{T}}]^{\mathrm{T}}. \tag{18}$$

Further,

$$\{q_n\} = [u_n\ \ w_n\ \ (\tau_{xz})_n\ \ (\sigma_z)_n]^{\mathrm{T}} \tag{19}$$

and

$$[N_n] = \begin{bmatrix} g_i f_q & -g'_i f_p & g_i f_p \dfrac{1}{D_{55}} & 0 \\ -g'_i f_p \dfrac{D_{13}}{D_{33}} & g_i f_q & 0 & g_i f_p \dfrac{1}{D_{33}} \end{bmatrix}. \tag{20}$$

n, i, q and p are same as expressed in equation (15). Furthermore,

$$g'_i = \frac{\partial g_i}{\partial x}. \tag{21}$$

In the absence of external and damping forces (i.e., undamped natural vibration), the total energy of an element within a lamina can be given by

$$L_e = T_e - U_e, \tag{22}$$

where U_e and T_e represent the internal strain and kinetic energies respectively. Functional in equation (22) can be expressed in the matrix form for linear elastic system as

$$L_e = \tfrac{1}{2}\left[\int \rho\{\dot{u}\}^{\mathrm{T}}\{\dot{u}\}\,\mathrm{d}v - \int \{\in\}^{\mathrm{T}}\{\sigma\}\,\mathrm{d}v\right], \tag{23}$$

where ρ is the mass density of the material, and

$$\{\dot{u}\} = \frac{\mathrm{d}\{u\}}{\mathrm{d}t}. \tag{24}$$

The strain vector $\{\in\}$ and the stress vector $\{\sigma\}$ can be expressed as

$$\{\in\} = [B]\{q\}, \tag{25}$$

$$\{\sigma\} = [D][B]\{q\}, \tag{26}$$

where

$$[B] = [\underline{B}_1\ \ \underline{B}_2\ \ \underline{B}_3\ \ \underline{B}_4\ \ \underline{B}_5\ \ \underline{B}_6] \tag{27}$$

and

$$[B_n] = \begin{bmatrix} \dfrac{\partial}{\partial x} & 0 \\ 0 & \dfrac{\partial}{\partial z} \\ \dfrac{\partial}{\partial z} & \dfrac{\partial}{\partial x} \end{bmatrix} [N_n] = \begin{bmatrix} g'_i f_q & -g''_i f_p & g'_i f_p \dfrac{1}{D_{55}} & 0 \\ -g'_i \bar{f}_p \dfrac{D_{13}}{D_{33}} & g_i \bar{f}_q & 0 & g_i \bar{f}_p \\ g_i \bar{f}_q - g''_i f_p \dfrac{D_{13}}{D_{33}} & g'_i (f_q - \bar{f}_p) & g_i \bar{f}_p \dfrac{1}{D_{55}} & g'_i \bar{f}_p \dfrac{1}{D_{33}} \end{bmatrix}. \quad (28)$$

n, i, q and p are the same as expressed in equation (15). Further,

$$g''_i = \frac{\partial^2 g_i}{\partial x^2} \quad \text{and} \quad \bar{f}_j = \frac{\partial f_j}{\partial z}, \; j = q \text{ or } p, \quad (29)$$

By summing up the total energies over all the elements and applying Hamilton's Principle [16]

$$\delta \int_{t_1}^{t_2} L \, \mathrm{d}t = 0, \quad (30)$$

where

$$L = \sum_e L_e \quad (31)$$

and δ implies first variation; the global equation of motion, in the absence of external forces, can be obtained as

$$[M]\{\ddot{Q}\} + [K]\{Q\} = 0. \quad (32)$$

Here global mass matrix $[M]$, global stiffness matrix $[K]$, and global nodal d.o.f. vector $\{Q\}$ are defined as

$$[M] = \sum_e [M]_e, \quad [K] = \sum_e [K]_e, \quad \{Q\} = \sum_e \{q\}, \quad (33)$$

where

$$[M_e] = \rho \int [N]^{\mathrm{T}} [N] \, \mathrm{d}v, \quad (34)$$

$$[K_e] = \int [B]^{\mathrm{T}} [D][B] \, \mathrm{d}v, \quad (35)$$

$$\{\ddot{Q}\} = \frac{\mathrm{d}^2 \{Q\}}{\mathrm{d}t^2}. \quad (36)$$

The general solution of the equation of motion (32) for harmonic vibrations can be considered of the form

$$\{Q\} = \{\hat{Q}\} \mathrm{e}^{\mathrm{i}\omega t}, \quad (37)$$

where $\{\hat{Q}\}$ is the modal vector and ω is the natural frequency. Substitution of equation (37) into equation (32) results in the following generalized eigenvalue problem:

$$([K] - \omega^2 [M])\{\hat{Q}\} = 0. \quad (38)$$

Solution of equation (38) yields the natural frequency ω and the corresponding eigenvector $\{\hat{Q}\}$ after the imposition of boundary conditions.

3. ILLUSTRATIVE EXAMPLES

A computer program incorporating the present two-dimensional mixed FE formulation has been developed in FORTRAN-90 to analyze natural vibrations of symmetric/unsymmetric composite laminated beams. Numerical computations have been performed for various examples. Results have been compared with the available analytical and FE solutions wherever these are available in the literature. Illustrative examples encompassing a couple of symmetric and unsymmetric cross-ply laminated beams under simple and clamped–free support conditions have been considered for highlighting the salient features of the model. The boundary conditions for various support conditions used in the analysis have been tabulated under Table 1. The geometrical and material properties as well as the lamination scheme for the examples are tabulated in Table 2.

The higher order FE solutions by Marur and Kant [17] and Kant *et al.* [18], and mixed theory by Rao *et al.* [19] have been considered for comparison of the results obtained in the present investigation. The present formulation was found to yield converging results by considering 8–10 elements along the X direction of the beam, along with the discretization of the thickness (i.e., along Z direction) in such a way, that the ratio L_x/L_z in an element was between 10 and 15.

The natural frequencies have been non-dimensionalized by using the expressions shown in Table 3 for a consistent comparison. Variations of normalized displacement ($\bar{u}$), in-plane normal stress ($\bar{\sigma}_x$), transverse shear and normal stresses ($\bar{\tau}_{xz}$ and $\bar{\sigma}_z$) through the thickness of beam under various bending, axial and shear modes of vibrations have been presented graphically, for simply supported thin and thick laminated beams (Data-1, Data-2 and Data-3 of Table 2). Normalization factors presented in Table 3 have been used for presenting the graphical results.

Illustrative numerical examples considered in the present work have been discussed next.

TABLE 1

Boundary conditions (BCs) applied to cross-ply laminated beams

Edge	BC on displacement field	BC on stress field0 >
Simple support condition		
(i) At $X=0$, a and $Z\neq 0$	$w=0$	—
(ii) At $X=0$ and $Z=0$	$u=w=0$	
(iii) At $Z=\pm d/2$	—	$\sigma_z=\tau_{xz}=0$
Clamped–free support condition		
(i) At $X=0$	$u=w=0$	—
(ii) At $X=a$	—	$\tau_{xz}=0$
(iii) At $Z=\pm d/2$	—	$\sigma_z=\tau_{xz}=0$
Clamped–simple support condition		
(i) At $X=0$ (clamped)	$u=w=0$	—
(ii) At $X=a$ (simple support)	$w=0$	—
(iii) At $Z=\pm d/2$	—	$\sigma_z=\tau_{xz}=0$
Clamped–clamped support condition		
(i) At $X=0$, a	$u=w=0$	—
(ii) At $Z=\pm d/2$	—	$\sigma_z=\tau_{xz}=0$
Partially clamped support conditions at both the ends (*only lower half of the vertical edges at both the ends are under clamped condition*)		
(i) At $X=0$, a and $Z=-d/2$ to 0	$u=w=0$	—
(ii) At $X=0$, a and $Z=0$ to $+d/2$	—	$\tau_{xz}=0$
(iii) At $Z=\pm d/2$	—	$\sigma_z=\tau_{xz}=0$

TABLE 2

Material properties data

Data no.	Properties	Description
Data-1 [18]	Geometrical properties	(1) Length $a = 15\,000$ mm (2) Breadth $b = 1000$ mm (3) Depth $d = 1000$ mm
	Material properties (material: AS4/3501-6/graphite/epoxy)	(1) $E_1 = 144{\cdot}80$ GPa (2) $E_2 = 9{\cdot}65$ GPa (3) $G = 4{\cdot}14$ Gpa (4) $v = 0{\cdot}3$ (5) $\rho = 1389{\cdot}23\text{E}{-}12\ \text{N s}^2/\text{mm}^4$
	Lamination scheme	$0°/90°/90°/0°$
Data-2 [18]	Geometrical properties	(1) Length $a = 762{\cdot}0$ mm (2) Breadth $b = 25{\cdot}4$ mm (3) Depth $d = 152{\cdot}4$ mm
	Material properties	(1) $E_1 = 525{\cdot}00$ Gpa (2) $E_2 = 21{\cdot}00$ Gpa (3) $G = 10{\cdot}50$ Gpa (4) $v = 0{\cdot}3$ (5) $\rho = 800{\cdot}00\text{E}{-}12\ \text{N s}^2/\text{mm}^4$
	Lamination scheme	$0°/0°/90°/90°/0°/0°$
Data-3 [17]	Geometrical properties	Same as Data-2.
	Material properties	Same as Data-2.
	Lamination scheme	$0°/90°/0°/90°/0°/90°$

TABLE 3

Normalization factor

Example no.	Normalization factor
All examples	$\bar{\omega} = \omega a^2 \sqrt{[\rho/(E_1 d^2)]}$ $\bar{Z} = \dfrac{Z}{d},\ \bar{u}(X,\bar{Z}) = \dfrac{u(X,\bar{Z})}{u(X,d/2)},\ \bar{\sigma}_x(X,\bar{Z}) = \dfrac{\sigma_x(X,Z)}{\sigma_x(X,d/2)}$
Example 1	$\bar{\tau}_{xz}(0,\bar{Z}) = \dfrac{\tau_{xz}(0,Z)}{\tau_{xz}(0,0)},\ \bar{\tau}_{xz}(a,\bar{Z}) = \dfrac{\tau_{xz}(a,Z)}{\tau_{xz}(a,d/4)},\ \bar{\sigma}_z(X,\bar{Z}) = \dfrac{\sigma_z(X,Z)}{\sigma_z(X,d/6)}$
Example 4	$\bar{\tau}_{xz}(0,\bar{Z}) = \dfrac{\tau_{xz}(0,Z)}{\tau_{xz}(0,0)},\ \bar{\tau}_{xz}(a,\bar{Z}) = \dfrac{\tau_{xz}(a,Z)}{\tau_{xz}(a,d/6)},\ \bar{\sigma}_z(X,\bar{Z}) = \dfrac{\sigma_z(X,Z)}{\sigma_z(X,d/6)}$
Example 5	$\bar{\tau}_{xz}(X,\bar{Z}) = \dfrac{\tau_{xz}(X,Z)}{\tau_{xz}(X,0)},\ \bar{\sigma}_z(X,\bar{Z}) = \dfrac{\sigma_z(X,Z)}{\sigma_z(X,d/3)}$

3.1. THIN-BEAM SECTIONS

Three examples on thin symmetric cross-ply laminated beam have been considered for natural vibration analysis. The geometrical and material properties as well as the lamination scheme for the beam are tabulated under Data-1 of Table 2.

3.1.1. *Example* 1

A symmetric cross-ply laminated (0°/90°/90°/0°) thin beam under simple support condition has been considered for free vibration analysis. The boundary conditions have been elaborated in Table 1. The non-dimensionalized natural frequencies ($\bar{\omega}$) obtained from the present investigation are compared in Table 4, with the first order beam theory (FOBT), higher order beam theories (HOBTs) [18] and the mixed theory [19]. Results have been observed to be in very good agreement with the HOBT and the mixed theory. Few new results of axial, bending and shear frequencies have also been presented in the table. The variation of normalized displacement $\bar{u}$, normal stresses $\bar{\sigma}_x$, $\bar{\sigma}_z$ and transverse shear stress $\bar{\tau}_{xz}$ through the thickness of the beam under various modes of vibration have been plotted in Figures 2, 3 and 4 respectively. Only the first, fifth and ninth bending modes have been presented in Figure 2 for brevity. The non-linear variation of displacement field, $\bar{u}$, through the thickness of the beam clearly illustrates that the FOBT would be unable to represent the higher bending modes, and any of the shear modes for both thin as well as thick laminated composite beams as it assumes linear variation of displacement field u through the thickness. Mode shapes showing the variation of transverse stress quantities τ_{xz} and $\sigma_z$through the thickness show continuity of these quantities at the layer interface with different material properties, which cannot be achieved by any of the displacement-based formulations, even using HOBTs. It can be observed from the variation of in-plane

TABLE 4

Comparison of non-dimensional natural frequencies of a simply supported thin symmetrically laminated composite beam (Data-1)

Mode	FOBT [18]	HOBT [18]	Mixed theory [19]	Present Study
Axial mode				
1	—	—	—	11·439(3)
2	—	—	—	39·493(7)
3	—	—	—	70·367(11)
4	—	—	—	99·837(14)
5	—	—	—	125·950(18)
Bending mode				
1	2·512	2·516	2·513	2·516(1)
2	8·589	8·669	8·660	8·673(2)
3	16·045	16·320	16·330	16·383(4)
4	23·795	24·371	24·436	24·613(5)
5	—	—	—	33·087(6)
6	—	—	—	41·827(8)
7	—	—	—	50·869(9)
8	—	—	—	57·907(10)
9	—	—	—	73·415(12)
10	—	—	—	85·748(13)
11	—	—	—	100·101(15)
12	—	—	—	116·524(16)
Shear mode				
1	—	—	—	119·522(17)
2	—	—	—	127·136(19)

Note. Value within brackets "() "indicates the mode number and "—" indicates result not available.

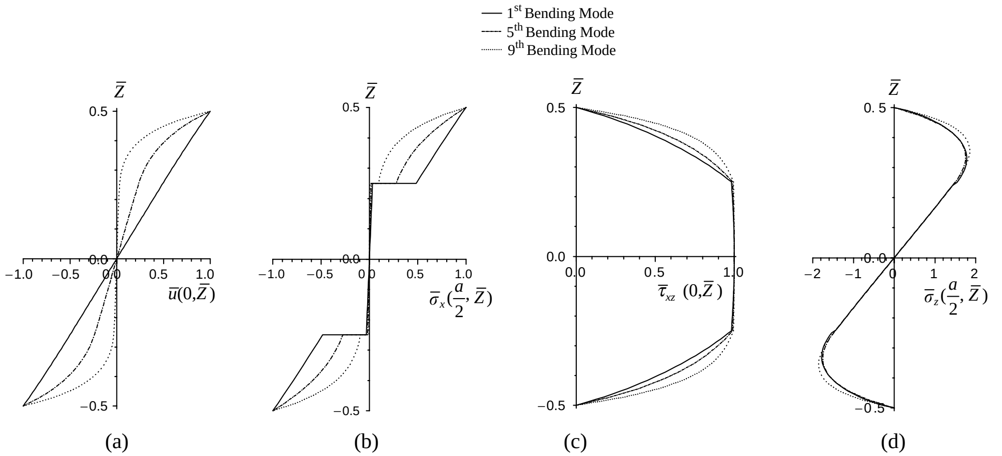

Figure 2. Through thickness variation of normalized (a) displacement ($\bar{u}$); (b) normal stress ($\bar{\sigma}_x$); (c) transverse shear stress ($\bar{\tau}_{xz}$); and (d) transverse normal stress ($\bar{\sigma}_z$) in various bending modes for a thin symmetric laminated beam (0°/90°/90°/0°).

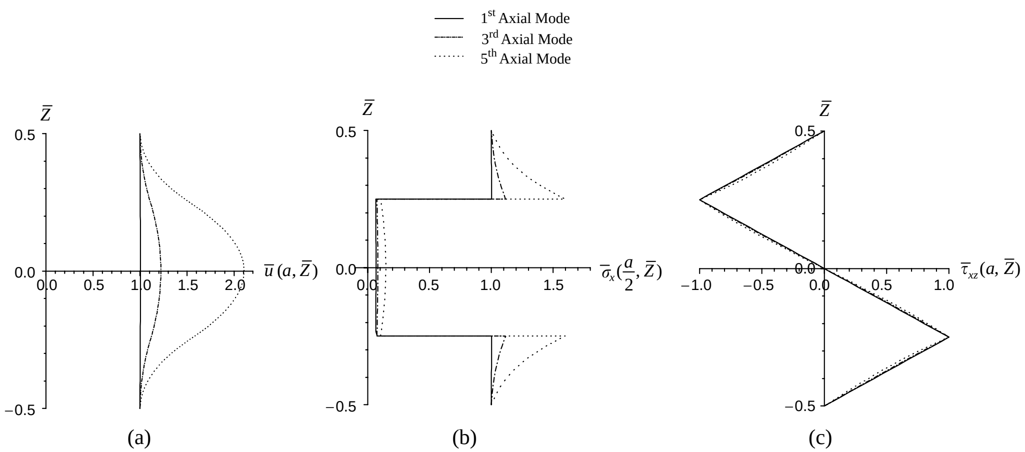

Figure 3. Through thickness variation of normalized (a) displacement ($\bar{u}$); (b) normal stress ($\bar{\sigma}_x$); and (c) transverse shear stress ($\bar{\tau}_{xz}$) in various axial mode for a thin symmetric laminated beam (0°/90°/90°/0°).

normal stress (σ_x) under bending mode of vibration, that the full depth of the top and bottom layers (which has high in-plane elastic modulus "E_1") effectively resists the moment even in higher modes of vibrations.

3.1.2. *Example* 2

The Beam in Example 1 has been considered under clamped–free support condition. The non-dimensionalized natural frequencies ($\bar{\omega}$) are presented in Table 5. Results from FOBT, HOBT (4a, 4b and 5) [17] and the mixed theory [19] have been considered for comparison of the results. The present models have been shown to yield results in good agreement with the results from HOBT (4b and 5). The possible reason for FOBT also giving good results, especially at low frequencies, can be attributed to the fact that the beam, which has a thin section, becomes quite flexible under the clamped–free support

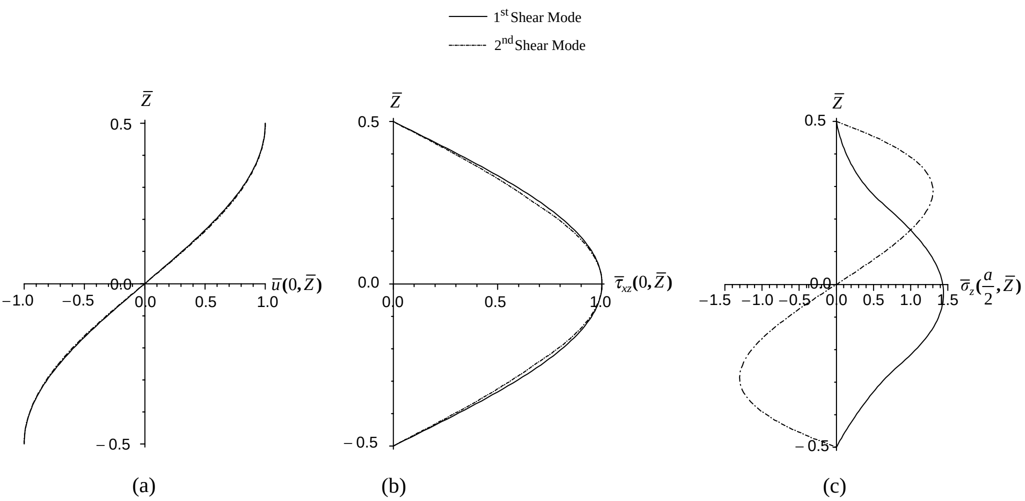

Figure 4. Through thickness variation of normalized (a) displacement ($\bar{u}$); (b) shear stress ($\bar{\tau}_{xz}$); and (c) transverse normal stress ($\bar{\sigma}_z$) in the first and second shear modes for a thin symmetric laminated beam (0°/90°/90°/0°).

TABLE 5

Comparison of non-dimensional natural frequencies of a clamped–free thin symmetrically laminated composite beam (Data-1)

Bending mode	FOBT [17]	HOBT4a [17]	HOBT4b [17]	HOBT5 [17]	Mixed theory [19]	Present study
1	0·923(1)	0·927(1)	0·924(1)	0·924(1)	0·923	0·925(1)
2	4·941(2)	5·073(2)	4·985(2)	4·985(2)	4·888	4·996(2)
3	11·656(3)	12·159(3)	11·832(3)	11·832(3)	11·433	11·879(3)
4	19·180(4)	20·262(4)	19·573(4)	19·573(4)	18·689	19·737(5)
5	27·038(5)	28·820(5)	27·720(5)	27·720(5)	26·203	28·174(6)
6	—	—	—	—	—	37·079(7)
7	—	—	—	—	—	46·632(8)
8	—	—	—	—	—	56·405(10)
9	—	—	—	—	—	68·855(11)
10	—	—	—	—	—	82·396(12)

Note. Value within brackets "()" indicates the mode number and "—" indicates result not available.

condition. However, the results from FOBT would be erroneous for vibration in higher modes due to the reduction in the effective flexibility. Natural frequencies for higher bending modes have also been presented in the table for future reference.

3.1.3. *Example* 3

The beam in Example 1 has been reconsidered to investigate variation in the natural frequencies under the following support conditions: (i) clamped–free; (ii) simple support at both the ends; (iii) clamped–simple; (iv) clamping in the lower half portion (i.e., partially clamped); and (v) clamped–clamped. The boundary conditions for all these different support conditions have been presented in Table 1. The first five non-dimensionalized natural frequencies ($\bar{\omega}$) are presented in Table 6, which can serve as benchmark solutions for future reference. The natural frequencies appear to be in consonance with the relative flexibility being provided to the beam by the different support conditions. Of course, the natural frequencies obtained under partially clamped support condition will depend on how much portion of the ends of the beam is under clamped support condition.

3.2. THICK-BEAM SECTIONS

One example on thick symmetric cross-ply laminated composite beam and one on thick unsymmetric laminated composite beam under simple support condition have been considered for natural vibration analysis.

3.2.1. *Example* 4

A six-layer symmetric cross-ply laminated ($0°/0°/90°/90°/0°/0°$) thick beam under simple support has been considered in this example. The geometrical and material properties for the beam correspond to Data-2 of Table 2. The non-dimensional frequencies in axial, bending and shear modes obtained through the present model have been compared in Table 7 with FOBT, HOBT (4a, b) [17], HOBT [18] and the mixed theory [19]. It can be observed that the results from the present studies are in good agreement with HOBT and the mixed theory. Through thickness variation of normalized displacement field $\bar{u}$, normal stress $\bar{\sigma}_x$ and transverse stress fields ($\bar{\tau}_{xz}$ and $\bar{\sigma}_z$) for bending, axial and shear modes have also been presented in Figures 5–7. Only the first, fifth and ninth bending modes have been presented in Figure 5 for brevity. It is interesting to observe that the variation of displacement field "u" is non-linear even for the first bending mode. Such predictions cannot be made by FOBT. Moreover, very high stress gradients have been observed in the variation of transverse shear and normal stresses at the faces of the beam, which obviously necessitates a refined theory such as the present one. Observation on the variation of in-plane normal stress $\bar{\sigma}_x$ reveals that unlike the thin-beam case of Example 1, a very small outer part of the top and bottom layers remains effective in resisting moments for higher modes of vibration. The through thickness continuity in the variation of transverse stresses at the layer interface as depicted in the figures marks the importance of mixed formulation over higher order displacement formulations.

TABLE 6

Comparison of non-dimensional natural frequencies of a thin symmetrically laminated composite beam under different support conditions (Data-1)

Bending mode	Support conditions				
	Clamped–free	Simple support	Clamped–simple	Partially clamped	Clamped–clamped
1	0·925	2·516	3·830	3·534	4·725
2	4·996	8·679	9·829	9·191	10·754
3	11·879	11·666	16·940	16·999	17·907
4	17·180	16·418	23·960	24·597	25·596
5	19·737	24·738	26·376	29·782	33·613

TABLE 7

Comparison of non-dimensional natural frequencies of a simply supported thick symmetrically laminated composite beam (Data-2)

Mode	FOBT [17]	HOBT4a [17]	HOBT4b [17]	HOBT [18]	Mixed theory [19]	Present study
Axial frequencies						
1	—	—	—	—	—	1·879(2)
2	12·953(8)	12·636(7)	12·953(7)	—	—	12·616(8)
3	25·910(14)	23·597(14)	25·910(14)	—	—	20·168(13)
Bending frequencies						
1	1·639(1)	1·736(1)	1·656(1)	1·657	1·654	1·655(1)
2	3·810(2)	4·125(2)	3·923(2)	3·910	3·916	3·908(3)
3	5·912(3)	6·439(3)	6·191(3)	6·138	6·180	6·146(4)
4	7·988(4)	8·722(4)	8·470(4)	8·323	8·446	8·400(5)
5	10·100(5)	11·042(5)	10·803(5)	10·440	10·771	10·694(6)
6	12·188(7)	13·333(8)	13·117(8)	12·469	12·969	13·061(9)
7	14·392(9)	15·751(9)	15·561(9)	14·385	15·222	15·510(10)
8	16·732(10)	18·313(10)	18·151(10)	16·161	17·469	17·404(11)
9	19·205(12)	21·021(12)	20·889(12)	17·771	19·712	21·639(14)
Shear frequencies						
1	11·181(6)	12·248(6)	11·111(6)	—	—	11·107(7)
2	19·088(11)	19·747(11)	18·927(11)	—	—	18·837(12)

Note. Value within bracket "( )" indicates the mode number and "—" indicates result not available.

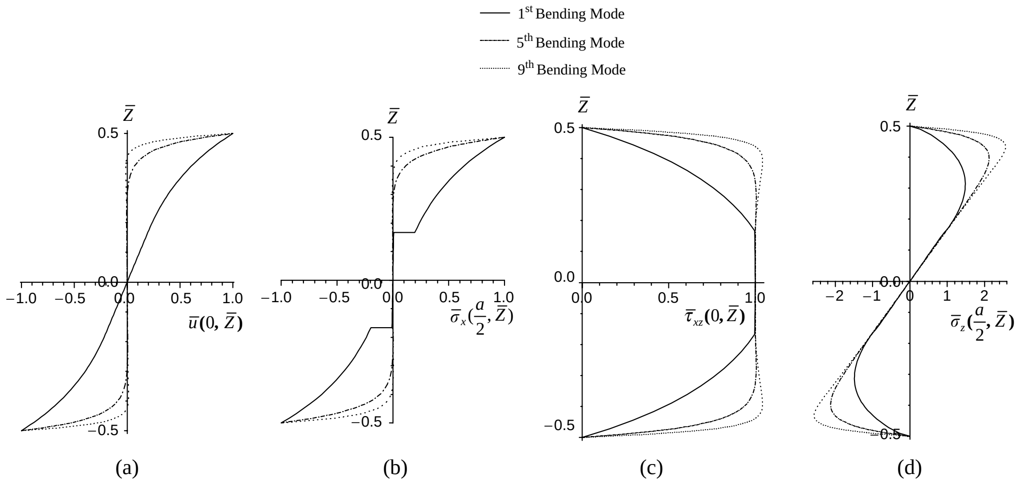

Figure 5. Through thickness variation of normalized (a) displacement ($\bar{u}$); (b) normal stress ($\bar{\sigma}_x$); (c) transverse shear stress ($\bar{\tau}_{xz}$) and (d) transverse normal stress ($\bar{\sigma}_z$) in various bending modes for a thick symmetric laminated beam (0°/0°/90°/90°/0°/0°).

3.2.2. *Example* 5

A six-layer unsymmetric cross-ply laminated (0°/90°/0°/90°/0°/90°) thick beam under simple support condition has been considered in this example. The geometrical and material properties are presented under Data-3 of Table 2. The non-dimensional natural frequencies ($\bar{\omega}$) for axial, bending and shear modes have been presented in Table 8. On the

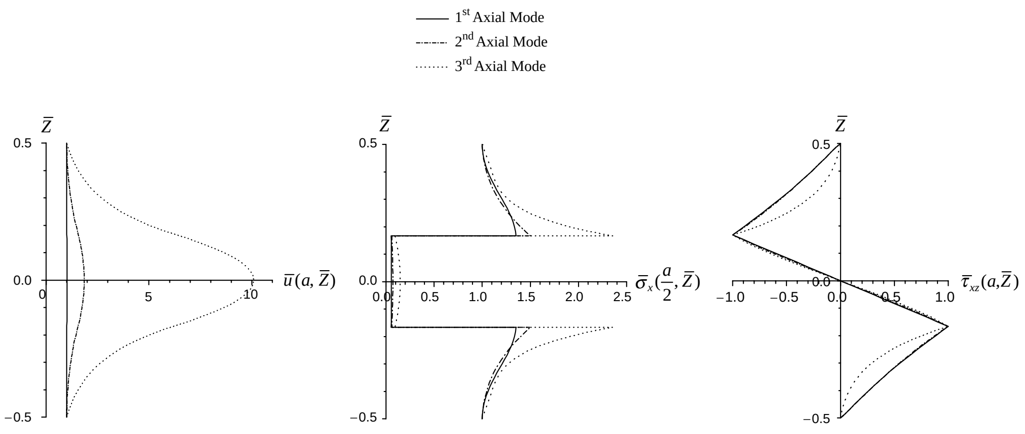

Figure 6. Through thickness variation of normalized (a) displacement ($\bar{u}$); (b) normal stress ($\bar{\sigma}_x$); and (c) transverse shear stress ($\bar{\tau}_{xz}$) in various bending models for a thick symmetric laminated beam (0°/0°/90°/90°/0°/0°).

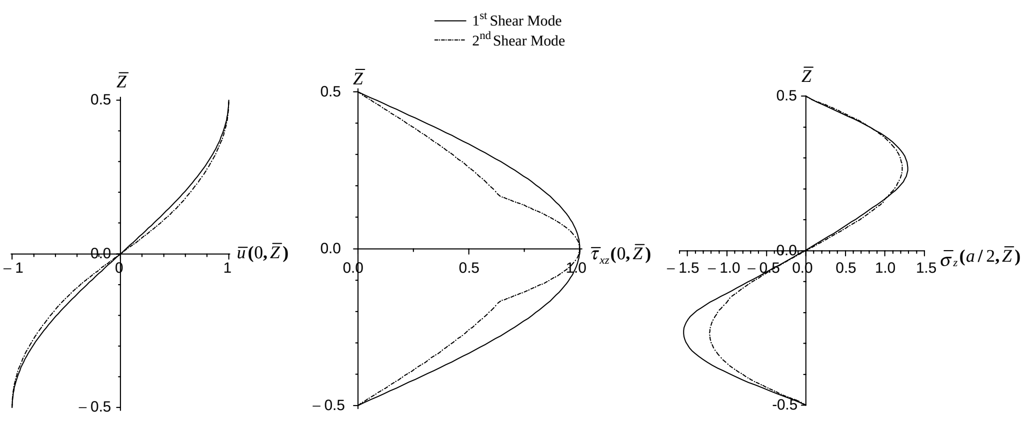

Figure 7. Through thickness variation of normalized (a) displacement ($\bar{u}$); (b) shear stress ($\bar{\tau}_{xz}$); and (c) transverse normal stress ($\bar{\sigma}_z$); in the first and second shear modes for a thick symmetric laminated beam (0°/0°/90°/90°/0°/0°).

other hand, the through thickness variation of in-plane displacement and various stress quantities under different types of modes are shown in Figures 8–10. Comparison of frequencies with the available results from FOBT and HOBT (4a, 4b, 5) [17] indicates that some of the natural frequencies obtained through the present formulation are somewhat lower than the corresponding results from FOBT and various HOBTs. Also, it has been conspicuously noted that FOBT and various HOBTs have failed to give the first axial mode of vibration in both the examples (i.e., Examples 4 and 5). It can be argued that a model based on equivalent single layer (ESL) displacement theory (viz., FOBT, HOBTs) cannot model precisely the exact behavior of a laminated composite member. On the other hand, the present mixed FE model satisfies exactly the important behavioral conditions of the continuity of displacement and transverse stress fields through the thickness of a

TABLE 8

Comparison of non-dimensional natural frequencies of a simply supported thick unsymmetrically laminated composite beam (0°/90°/0°/90°/0°/90°) (Data-3)

Mode	FOBT [17]	HOBT4a [17]	HOBT4b [17]	HOBT5 [17]	Present study
Axial frequencies					
1	—	—	—	—	2·791(2)
2	10·932(6)	10·935(6)	10·762(6)	10·668(6)	11·597(8)
3	21·855(14)	21·709(13)	21·430(13)	21·108(13)	19·294(13)
Bending frequencies					
1	1·432(1)	1·483(1)	1·434(1)	1·416(1)	1·376(1)
2	3·597(2)	3·806(2)	3·614(2)	3·531(2)	3·480(3)
3	5·750(3)	6·153(3)	5·870(3)	5·675(3)	5·577(4)
4	7·856(4)	8·457(4)	8·114(4)	7·795(4)	7·696(5)
5	9·994(5)	10·809(5)	10·462(5)	10·021(5)	9·887(6)
6	12·104(8)	13·132(8)	12·807(8)	12·285(8)	12·189(9)
7	14·319(9)	15·575(9)	15·253(9)	14·633(9)	14·062(10)
8	16·673(11)	18·166(11)	17·873(11)	17·244(11)	16·178(12)
9	19·147(12)	20·889(12)	20·611(12)	19·981(12)	20·314(14)
Shear frequencies					
1	11·181(7)	12·248(7)	11·110(7)	11·110(7)	11·107(7)
2	15·868(10)	16·468(10)	15·839(10)	15·663(10)	15·871(11)

Note. Value within bracket "()" indicates the mode number.

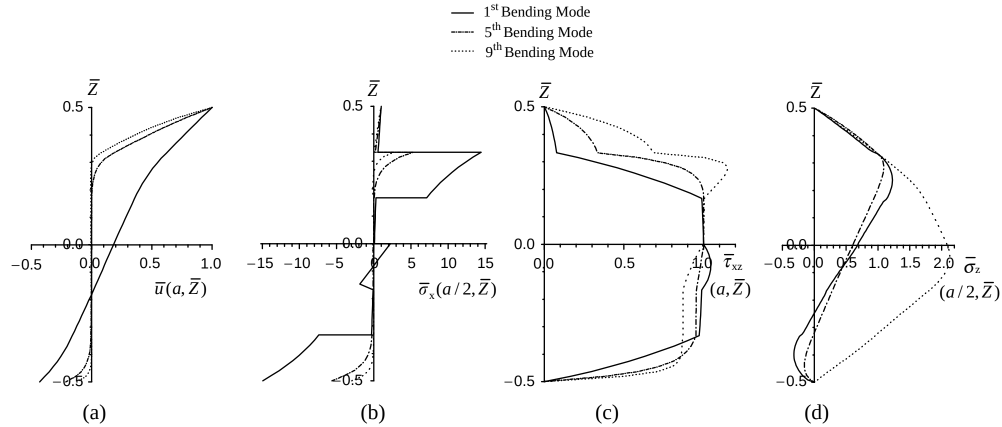

Figure 8. Through thickness variation of normalized (a) displacement ($\bar{u}$); (b) normal stress ($\bar{\sigma}_x$); (c) transverse shear stress ($\bar{\tau}_{xz}$) and (d) transverse normal stress ($\bar{\sigma}_z$) in various bending modes for a thick unsymmetric laminated beam (0°/0°/90°/90°/0°/0°).

laminated composite beam. Because the present example consists of five interfaces with abrupt change in the material properties compared to the previous examples having only two, the displacement-based ESL models are unable to incorporate abrupt changes properly into their formulation. On the other hand, the present mixed formulation has the ability to model the sudden changes in the material properties very efficiently.

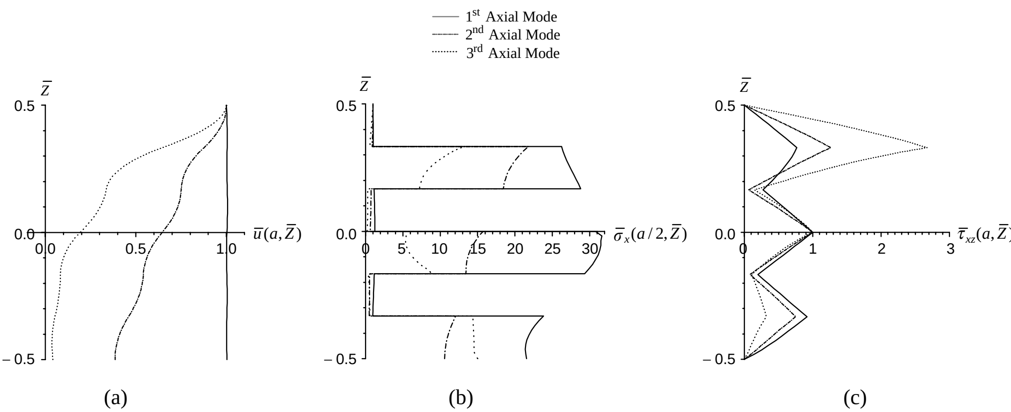

Figure 9. Through thickness variation of normalized (a) displacement ($\bar{u}$); (b) normal stress ($\bar{\sigma}_x$); and (c) tyransverse shear stress ($\bar{\tau}_{xz}$) in various axial mode for a thick unsymmetric laminated beam (0°/0°/90°/90°/0°/0°).

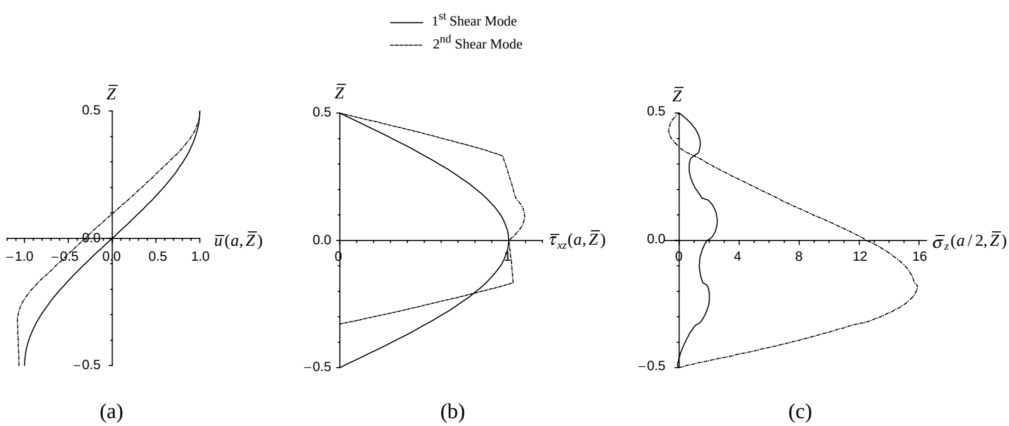

Figure 10. Through thickness variation of normalized (a) displacement ($\bar{u}$); (b) shear stress ($\bar{\tau}_{xz}$); and (c) transverse normal stress ($\bar{\sigma}_z$) in the first and second shear modes for a thick unsymmetric laminated beam (0°/0°/90°/90°/0°/0°).

4. CONCLUSIONS

A novel methodology for the formulation of mixed finite element (FE) model has been presented in this paper. The FE model has been developed by maintaining the fundamental elasticity relationship between constituents of the stress, strain and displacement fields within the elastic continuum. Because it is a layer-wise FE formulation with the transverse stress components as the degrees of freedom at the nodes, both the primary requirements of the continuity of displacement fields, as well as those of transverse stress components through the thickness of the beam have been satisfied. A comparison of the natural frequencies with various FE and mixed analytical models reveal that the formulation is well capable of dealing with laminated composite beam problems under different conditions of supports and loadings. The figures showing the variation of transverse normal and shear stresses through the thickness of laminated beams clearly depict the presence of high stress gradients, particularly at higher modes of vibrations. The present formulation has shown its ability in handling such problems.

ACKNOWLEDGMENTS

The constructive comments of reviewers are gratefully acknowledged.

REFERENCES

1. R. B. Pipes and N. J. Pagano 1970 *Journal of Composite Materials* **4**, 538–548. Interlaminar stresses in composite laminates under uniform axial loading.
2. E. F. Rybicki 1971 *Journal of Composite Materials* **5**, 354–360. Approximate three-dimensional solutions for symmetric laminates under in-plane loading.
3. R. M. Jones 1975 *Mechanics of Composite Materials*. Tokyo: McGraw-Hill, Koga Kusha, Ltd.
4. S. Srinivas and A. K. Rao 1970 *International Journal of Solids and Structures* **6**, 1463–1481. Bending vibration and buckling of simply supported thick orthotropic rectangular plates and laminates.
5. N. J. Pagano 1970 *Journal of Composite Materials* **4**, 20–35. Exact solutions for rectangular bi-directional composites and sandwich plates.
6. N. J. Pagano and S. J. Hatfield 1972 *American Institute of Aeronaectics and Astronautics Journal* **10**, 931–933. Elastic behavior of multilayered bi-directional composites.
7. J. N. Reddy 1987 *Communications in Applied Numerical Methods* **3**, 173–180. A generalization of two-dimensional theories of laminated composite plates.
8. K. P. A. Soldatos 1992 *Composite Structures* **20**, 195–211. A general laminated plate theory accounting for continuity of displacements and transverse shear stresses at material interfaces.
9. C. P. Wu and H. C. Kuo 1993 *Composite Structures* **24**, 29–42. An interlaminar stress mixed finite element method for the analysis of thick laminated composite plates.
10. C. P. Wu and C. S. Hsu 1993 *Composite Structures* **25**, 439–448. A new local high-order laminate theory.
11. C. P. Wu and C. C. Lin 1993 *Composite Structures* **25**, 397–405. Analysis of sandwich plates using mixed finite element.
12. Y. B. Shi and H. R. Chen 1992 *Composite Structures* **20**, 127–136. A mixed finite element for interlaminar stress computation.
13. E. Carrera 1996 *International Journal of Numerical Methods in Engineering* **39**, 1179–1820. C^0 Reissner–Mindlin multilayered plate elements including zig-zag and interlaminar stress continuity.
14. E. Carrera 1998 *Composite Structures* **43**, 57–70. Mixed layer-wise models for multilayered plates analysis.
15. E. Carrera 1999 *ASME Journal of Applied Mechanics* **66**, 1004–1011. Transverse normal stress effects in multilayered plates.
16. K. J. Bathe 1997 *Finite Element Procedures*. New Delhi: Prentice-Hall of India.
17. S. R. Marur and T. Kant 1996 *Journal of Sound and Vibration* **194**, 337–351. Free vibration analysis of fiber-reinforced composite beams using higher order theories and finite element modeling.
18. T. Kant, S. R. Marur and G. S. Rao 1998 *Composite Structures* **40**, 1–9. Analytical solution to the dynamic analysis of laminated beams using higher order refined theory.
19. M. K. Rao, Y. M. Desai and M. R. Chitnis 2001 *Composite Structures* **52**, 149–160. Free vibrations of laminated beams using mixed theory.